NASA Technical Memorandum 104138

MAXIMIZED GUST LOADS FOR A NONLINEAR AIRPLANE USING MATCHED FILTER THEORY AND CONSTRAINED OPTIMIZATION

Robert C. Scott, Anthony S. Pototzky, and Boyd Perry III

September 1991

National Aeronautics and Space Administration

Langley Research Center
Hampton, Virginia 23665-5225

Maximized Gust Loads For a Nonlinear Airplane Using Matched Filter Theory and Constrained Optimization

By

Robert C. Scott ♠

Anthony S. Pototzky ♦

and

Boyd Perry, III ♣

Abstract

This paper describes and illustrates two matched-filter-theory based schemes for obtaining maximized and time-correlated gust-loads for a nonlinear airplane. The first scheme is computationally fast because it uses a simple one-dimensional search procedure to obtain its answers. The second scheme is computationally slow because it uses a more complex multi-dimensional search procedure to obtain its answers, but it consistently provides slightly higher maximum loads than the first scheme. Both schemes are illustrated with numerical examples involving a nonlinear control system.

Nomenclature

BM	bending moment
exc(t,p)	iterative excitation waveform time history obtained from optimization design variables (p)
F(p)	objective function
g(p)	constraint function
k	impulse strength
KS(p)	Kreisselmeier Steinhauser function
i	iteration number
p	vector of design variables
RMS	root mean square
RMS(x)	root mean square of quantity x
t	time
TM	torsion moment
t_0	arbitrary time shift
WOBTM	wing outboard torsion moment
WRBM	wing root bending moment
y(t)	time response of output quantity y
y(t,p)	time response of output quantity y to iterative excitation waveform
$y_h(t)$	time response of output quantity y to an impulse
$y_y(t)$	time response of output quantity y to excitation matched to y
z(t)	time response of output quantity z
$z_y(t)$	time response of output quantity z to excitation matched to y
ρ	scalar multiplying factor used in the KS function
σ_g	root-mean-square of gust velocity

♠ NASA Langley Research Center, Structural Dynamics Division; Member AIAA.

♦ Lockheed Engineering and Sciences Company; Member AIAA.

♣ NASA Langley Research Center, Structural Dynamics Division.

Introduction

Time-correlated gust loads are time histories of two or more load quantities due to the same disturbance time history. Time correlation provides knowledge of the value (magnitude and sign) of one load when another is maximum. Figure 1 contains an illustration of time-correlated gust loads. At least two analysis methods have been identified (refs. 1 and 2) that are capable of computing maximized time-correlated gust loads for linear aircraft. Both methods solve for the gust profile (gust velocity as a function of time) that produces the maximum load at a given location on a linear airplane. Time-correlated gust loads are obtained by re-applying this gust profile to the airplane and computing multiple simultaneous load responses. The load responses are physically realizable at all instants of time during the time history (including the instant at which a given load is maximum), and correlated loads at any of these instants may be applied to aircraft structures.

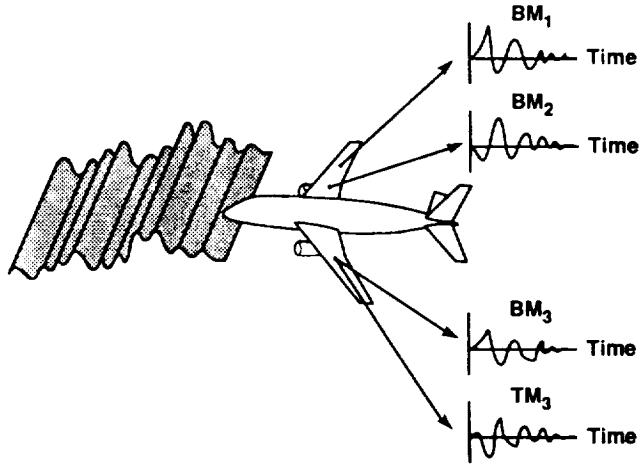

Figure 1.- Time-correlated gust loads.

Within the past several years there has been much interest in obtaining a practical analysis method that is capable of solving the analogous problem for nonlinear aircraft. Such an analysis method, and the broader issues of harmonizing existing criteria and minimizing the number of different analyses required for certification, have been the on-going focus of an international committee of gust loads specialists formed by the U. S. Federal Aviation Administration (ref. 3). The method of reference 1 is capable of being, but so far has not been, applied to nonlinear aircraft. As stated in reference 1, to make the method practical for nonlinear applications, a search procedure is essential. The method of reference 2 is based on Matched Filter Theory (MFT) and, in its current form, is applicable to linear systems only.

The purpose of the present paper is to extend the method described in reference 2 to nonlinear systems. The extension uses MFT as a starting point and then employs a constrained optimization algorithm to attack the nonlinear problem. Reference 4 contains a status report (as of April 1990) on the development of this extension. In the present paper, methodology development is refined and completed and numerical results are presented that illustrate an application of the method to an airplane with a nonlinear control system.

Review of Matched Filter Theory For Linear Systems

As background for the remainder of this paper, this section presents the key results from reference 2, the original development of MFT for computing maximized and time-correlated gust loads for linear airplanes.

Figure 2 depicts the steps that must be employed to implement MFT and illustrates the intermediate and final products of the process. Frequency-response-function representations of atmospheric turbulence and airplane loads are combined in series and represent the "known dynamics" boxes in the figure. One-dimensional Gaussian atmospheric turbulence with the von Karman power spectrum is chosen. Load y is the load to be maximized. Loads z_1 through z_n are the loads to be time correlated with load y. There are three major steps in the process:

Step 1 The application of an impulse function of unit strength to the combined linear system, producing the impulse response of load y.

Step 2 The normalization of this impulse response by its own RMS value, followed by its reversal in time.

Step 3 The application of this normalized reversed signal to the combined linear system, producing time histories of load y and time histories of loads z_1 through z_n. Within the time history of load y, the maximum value is y_{max}.

For simplicity of discussion throughout this paper, these three steps will be referred to as "linear MFT." Within each step, significant results, interpretations, and implications are:

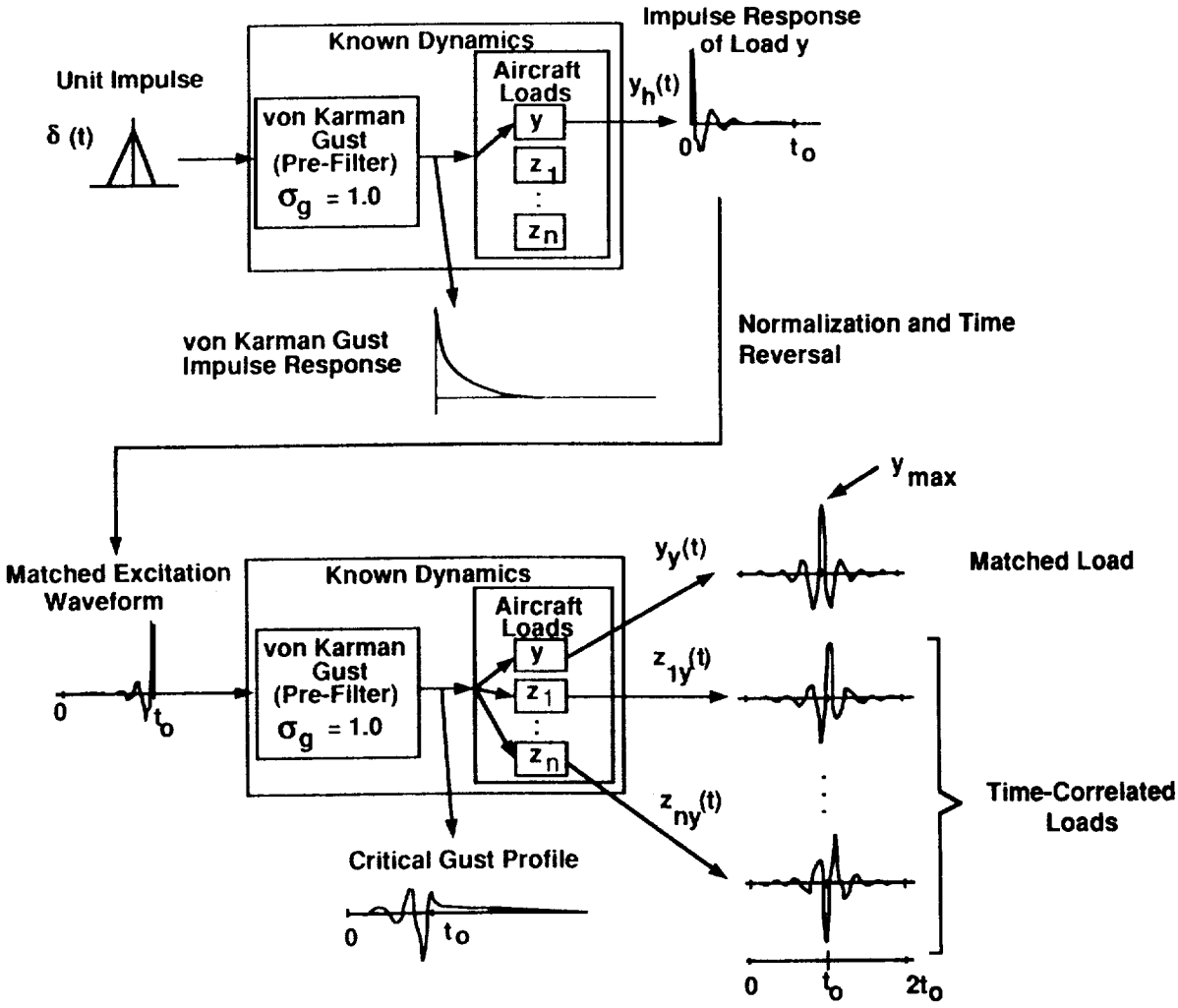

Figure 2.- Schematic for linear matched filter theory.

Within Step 1 The impulse response of atmospheric turbulence is shown as an intermediate quantity. The impulse responses of loads z_1 through z_n can be computed but are not used.

Within Step 2 The normalized reversed signal, named the matched excitation waveform, now has a unit RMS value. MFT guarantees that there is no other unit-RMS excitation waveform that, when applied to the combined linear system, will produce a value of y larger than y_{max}. This guarantee is a fundamental result of MFT.

Within Step 3 The response of atmospheric turbulence to the matched excitation waveform, named the critical gust profile, has a given level of probability. The responses of atmospheric turbulence to all other unit-RMS excitation waveforms have the same given level of probability. Load y is named the matched load and loads z_1 through z_n are time correlated with load y. At each instant of time, the time history of the matched load is proportional to the autocorrelation function of load y from a conventional random process analysis. At each instant of time, the time histories of loads z_1 through z_n are proportional to their corresponding cross-correlation functions with load y.

For more detailed information about the application of MFT to the calculation of maximized and time-correlated gust loads, including background, theoretical development, numerical implementation, and example calculations, the reader is urged to consult reference 2.

The Application of Matched Filter Theory to Nonlinear Systems

The goal of MFT as applied to nonlinear systems is the same as that for linear systems: to find the maximized response time history, the maximum value of the response within that time history, and the time-correlated response time histories. Because the system is now nonlinear, superposition and other convenient features of linear MFT no longer hold, the most convenient being that problems can be solved directly. For nonlinear systems, problems cannot be solved directly and a search procedure is the only practical means of finding the solution. Here "the solution" means searching for and finding the excitation waveform that maximizes y_{max}. The search is conducted systematically, subject to the constraint that the excitation waveform have unit RMS, using the techniques of numerical optimization.

Because superposition no longer holds, the magnitude and character of the responses are not necessarily proportional to the magnitude of the input. For the remainder of this paper two input magnitudes are important: k, the strength of the initial impulse; and σ_g, the design value of the gust intensity. (For linear MFT, the magnitude of both of these quantities was unity.) For nonlinear systems the shape of the excitation waveform is a function of k and σ_g, and, consequently, the quantity y_{max} is also a function of these parameters.

This section of the paper is divided into two subsections. The first describes a one-dimensional search procedure and the second describes a multi-dimensional search procedure. The original goal of the present research was to develop the multi-dimensional search only. However, in an effort to choose a reasonable starting point for the multi-dimensional search the authors happened upon the one-dimensional search, and as will be shown in the numerical results section of this paper, the one-dimensional search turned out to be a valuable procedure in its own right.

One-Dimensional Search Procedure

The one-dimensional search procedure performs a systematic variation of the quantity k to find the shape of an excitation waveform that maximizes y_{max}. Figure 3 contains a signal flow diagram for this search procedure. Figure 3 is very similar to figure 2, but contains some subtle yet important differences that are indicated by the shaded boxes and by quotation marks. In figure 3 the initial impulse has a non-unity strength; the aircraft loads portion of the known dynamics box contains nonlinearities; and the shape of the excitation waveform and the value of y_{max} are functions of the initial impulse strength. In addition, the "matched" excitation waveform and the "matched" load are shown in quotes because, for nonlinear systems, there is no guarantee that y_{max} is a global maximum.

The application of the one-dimensional search procedure is as follows:

Step 1 Select a design value of σ_g.

Step 2 Select a range of values of k.

Step 3 For each value of k, perform steps 1 through 3 of linear MFT, obtaining values of y_{max} and corresponding "matched" excitation waveforms.

Step 4 From step 3 above, find the maximum value of y_{max} and its corresponding "matched" excitation waveform.

Multi-Dimensional Search Procedure

The multi-dimensional search procedure uses as its starting point the maximum value of y_{max} and the corresponding "matched" excitation waveform obtained by performing the one-dimensional search procedure. In an attempt to obtain an even larger value of y_{max}, the shape of the "matched" excitation waveform is further optimized subject to the unit-RMS constraint mentioned above. The major features of this optimization procedure are illustrated in figure 4.

Initial excitation waveform. - Beginning in the upper left corner of figure 4, the box labelled initial excitation waveform is the waveform resulting from the one-dimensional search procedure.

Coefficient generator. - The purpose of the "coefficient generator" is to approximate the initial excitation waveform by a finite number of coefficients. These coefficients are first used as the design variables in the optimization procedure and later used to "reassemble" the final optimized waveform time history. Because the execution time of the optimization procedure is roughly proportional to the number of design variables, an important consideration was to choose an approximation technique that produced in the smallest number of coefficients for a given goodness of approximation. Several approximation techniques were considered including the use of orthogonal functions and cubic splines.

The orthogonal functions considered were Fourier series and Chebyshev polynomials. It was found (ref. 4) that it took about an order of magnitude fewer coefficients to approximate the initial excitation waveform with Chebyshev polynomials than to approximate it with Fourier series. Figure 5 shows an initial excitation waveform and approximations to it using first a 20-

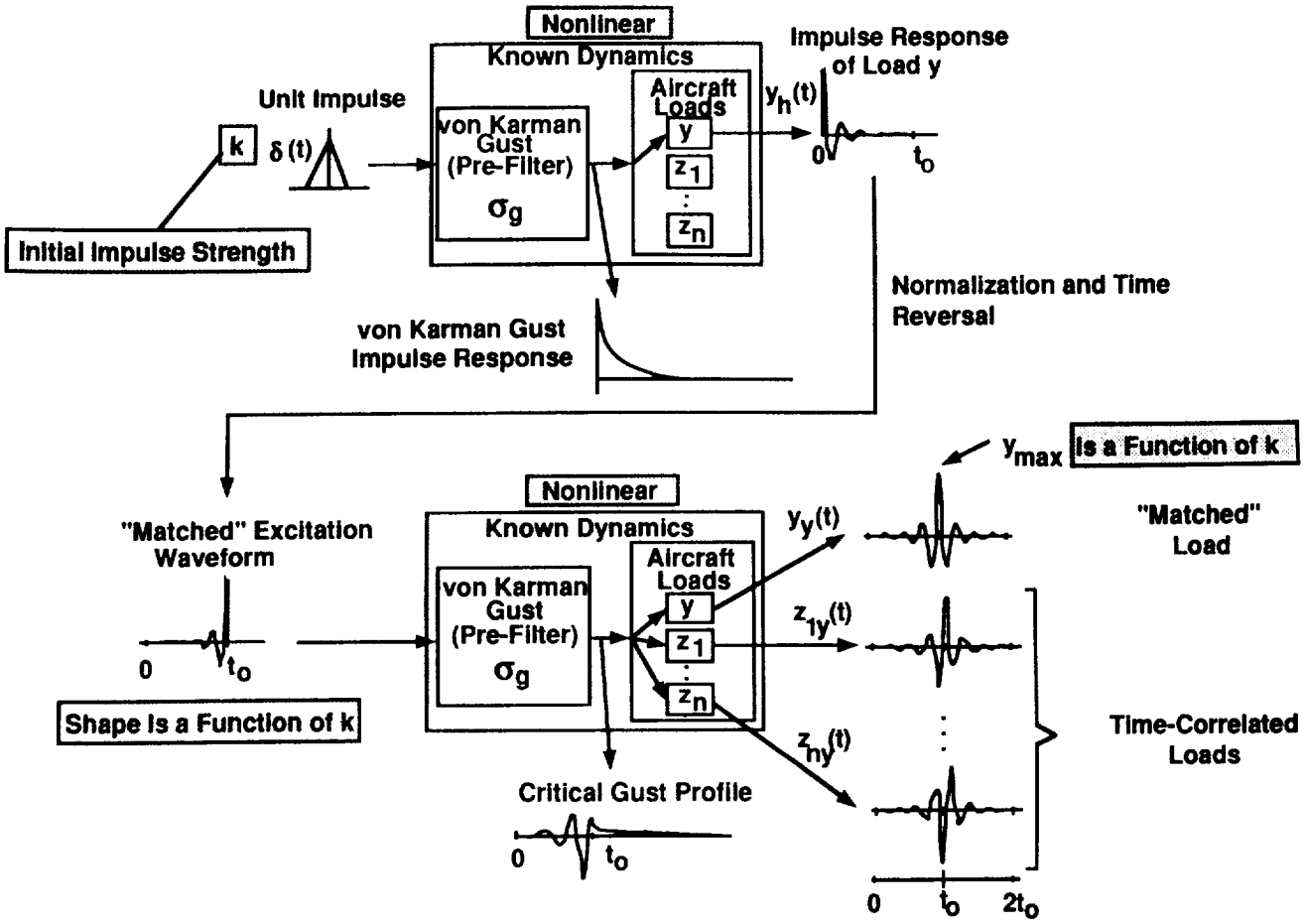

Figure 3.- Schematic for one-dimensional search procedure.

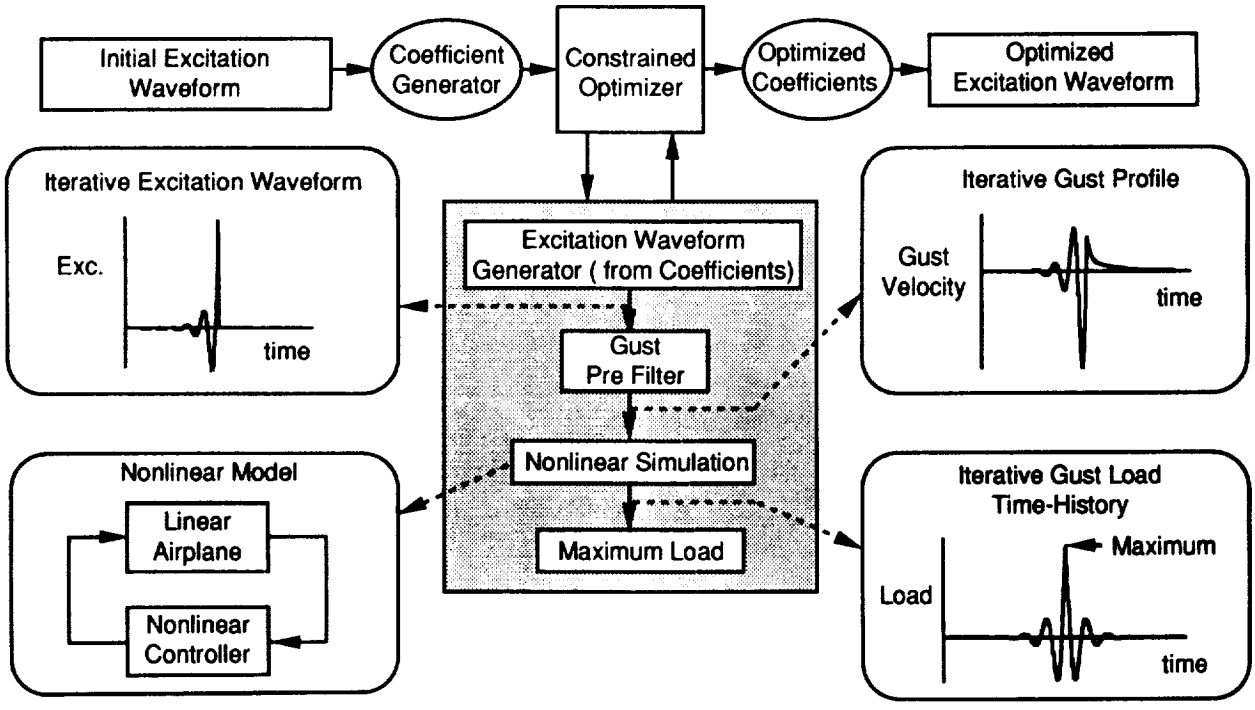

Figure 4.- Schematic for multi-dimensional search procedure.

term and then a 54-term Chebyshev approximation. The choice of how many coefficients to include in the approximation was made by examining a plot of the absolute value of the coefficient versus the coefficient number.

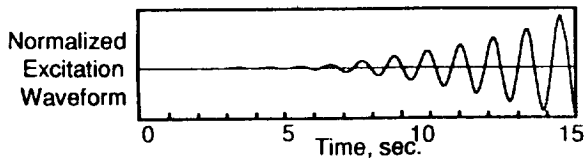

(a) Original excitation waveform.

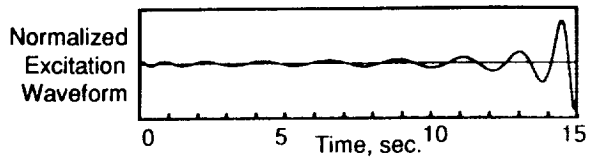

(b) Chebyshev approximation using 20 terms.

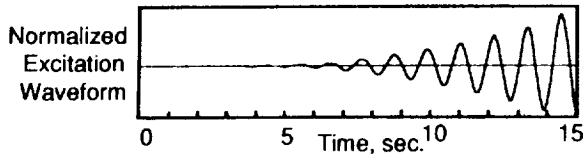

(c) Chebyshev approximation using 54 terms.

Figure 5.- Excitation waveform approximations using Chebyshev polynomials.

A waveform approximation technique based on cubic splines was also considered. For this method, discrete points in the waveform time-history were selected as design variables. The amplitudes of these points could then be changed by the optimization routine. By using a cubic spline the waveform time history can be assembled from these discrete points as needed in the optimization algorithm. As will be shown, this technique did not provide as accurate an approximation as Chebyshev polynomials, yet the number of design variables could be substantially reduced.

Constrained optimization algorithms. - Two optimization algorithms were considered: a direct method and an indirect method. This section briefly describes these algorithms.

The direct method (ref. 5) chooses search directions (systematic variations of the values of the coefficients) that minimize an objective function without violating constraints. The objective of this particular application is to maximize one of the loads. This objective function is formulated such that increasing the load, maximizing wing root bending moment (WRBM) for instance, reduces the objective function.

$$\text{Objective: minimize } F(p) = -\{ \max_{\text{over all } t} [\, y(t,p) \,] \}^2 \qquad (1)$$

The only constraint is that of keeping the RMS of the excitation waveform, exc(t,p), at or below a specified value. In actuality the waveform RMS should remain constant, implying the necessity for an equality constraint. However, in practice an inequality constraint performs very well, with the optimizer driving the value of the constraint to its maximum-allowable value. This, in effect, gives the desired result while not overly constraining the design space.

$$\text{Constraint: } g(p) = \{RMS[\, exc(t,p) \,] - 1.0\} \le 0.0 \qquad (2)$$

The indirect method (ref. 6) converts a constrained optimization problem into an unconstrained problem by combining the constraints with the objective functions into a single composite function known as the Kreisselmeier-Steinhauser function. The KS function is formulated such that it decreases when the objective function increases and increases when the constraint is violated. Here, the optimizer varies the coefficients to minimize the KS function.

$$KS(p) = \frac{1}{\rho} \log_e \left[\exp\left(\rho \left\{ (g(p_{i-1}) + 1 - \frac{F(p_i)}{F(p_{i-1})} \right\}\right) + \exp(\rho\, g(p_i)) \right] \qquad (3)$$

where F and g are defined in equations (1) and (2).

The shaded box in figure 4 contains the detailed sequential analysis steps performed. The optimizer cycles through the shaded box many times per iteration to obtain gradient information. The accompanying illustrations in the figure (boxes with rounded corners) show intermediate results and the nonlinear model.

Nonlinear simulation. The most computationally expensive aspect of this multi-dimensional search is the nonlinear simulation, shown in the shaded box in figure 4. The original simulation model was written in MATRIX$_x$ SYSTEM_BUILD simulation language (ref. 7). This high-level language proved very slow considering the large number of simulations required by the optimization algorithms. Therefore, the entire process was converted to FORTRAN with the code for the simulation model being created by MATRIX$_x$ HYPER_BUILD (ref. 8). This greatly increased throughput so that optimization results could be obtained in a reasonable amount of time. In addition, double precision was used so that sufficiently accurate gradient information could be obtained from the simulations.

Numerical Results

This section presents numerical results for the one-dimensional and multi-dimensional search procedures.

Example System

A nonlinear simulation model of the ARW-2 drone aircraft equipped with a nonlinear control system was constructed to demonstrate both search procedures. Figure 6 shows a block diagram of the simulation model and includes the aeroelastic plant, a gust load alleviation (GLA) control law, and nonlinear control elements. The aeroelastic plant is a linear, s-plane aeroelastic half-model consisting of two symmetric rigid-body modes and three flexible modes. Unsteady aerodynamics were obtained using the doublet lattice method (ref. 9). The model also includes the dynamics of the control surface actuators. The two-input/two-output GLA control law was

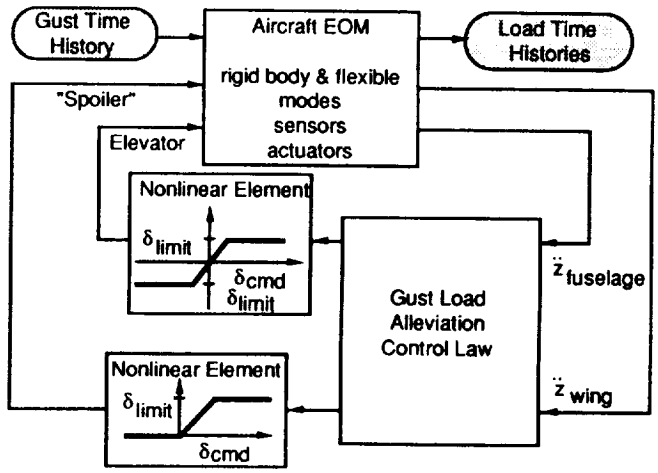

Figure 6.- Nonlinear model of aircraft and gust load alleviation system.

obtained using a Linear Quadratic Gaussian design approach with the intent of reducing wing root bending moment (ref. 10). The nonlinear elements impose deflection limits of ±10° on the elevators and 0 to +10° on the ailerons, simulating spoilers.

Two versions of this model will be considered: a simple version having only rigid-body modes (10 states) that served as a computationally economical test case; and a much larger, fully flexible model (32 states). These models will be hereinafter referred to as the rigid and flexible models, respectively. Analysis conditions for this model are 0.86 Mach number and 24,000 feet altitude.

One-Dimensional Search

The one-dimensional search procedure was performed on the rigid model. In order for the control-surface deflection limits to become active in the simulation, an artificially large value of gust intensity, σ_g, was required. With this value chosen, values of the initial impulse strength, k, were selected over the range from 0.1 to 1000. Typical results, in this case corresponding to maximizing wing root bending moment (WRBM), are presented in figure 7. Figure 7 contains 3 plots. The lower portion of the figure contains a plot of WRBM as a function of initial impulse strength: the solid circles are actual numerical results; the solid line is a faired line. Three sets of time histories of excitation waveform and its associated maximized WRBM are shown in the upper portion of figure 7. The corresponding values of k are indicated on the figure. For this particular example, a value of k of about three yields the largest maximized value of WRBM.

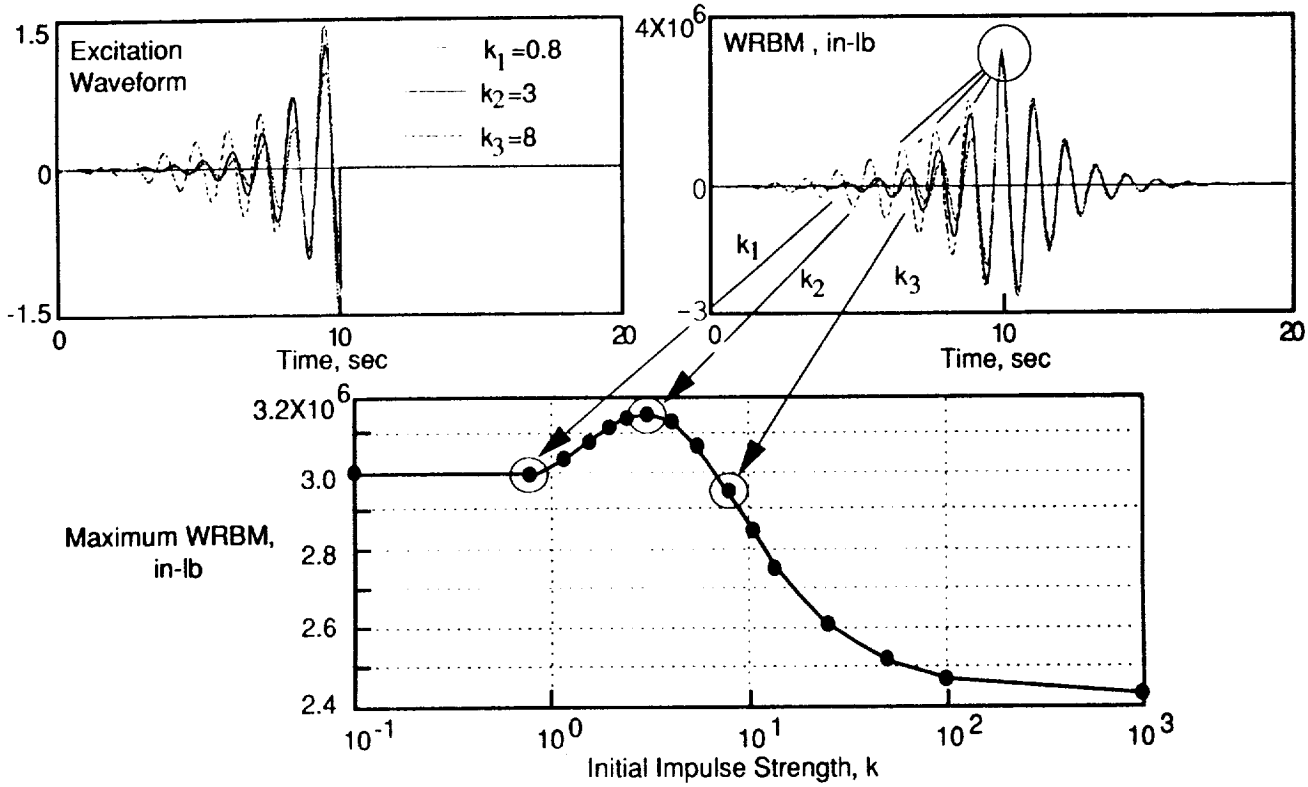

Figure 7.- Results from one-dimensional search procedure. Rigid model.

Multi-Dimensional Search

Maximizing WRBM in the rigid model will again be considered. To more clearly demonstrate the method, a nonoptimal value of k (k_1) was chosen to obtain the initial excitation waveform for this example. The Chebyshev waveform approximation was utilized in this example and required 54 coefficients (design variables). The direct optimizer was used and the resulting convergence history is shown in figure 8. This figure shows that the optimization scheme succeeds in increasing the maximum WRBM while ultimately satisfying the RMS constraint on the excitation waveform.

Figure 9 shows a comparison of the initial and optimized time histories for this test case. By considering figures 8 and 9, two conclusions can be drawn: (1) the multi-dimensional search procedure succeeds in altering the shape of the excitation waveform which causes alterations of the various time-histories and an increase in the maximum WRBM; and (2) the procedure achieves this increase in maximum load while maintaining the RMS constraint on the excitation waveform.

Figure 10 presents the results of applying the multi-dimensional search procedure a number of times. Again WRBM is the load of interest and again the rigid model is employed. The direct and indirect optimizers were exercised and excitation waveforms were approximated by Chebyshev polynomials and by cubic splines. The numbers in parentheses indicate the number of terms required to obtain an acceptable approximation to the waveform. The solid line in figure 10 is the faired line presented originally in figure 7. For the example shown, the direct optimizer with the Chebyshev polynomials was the best combination for reproducing the results from the one-dimensional search procedure and for obtaining the largest maximized loads.

The squares and circles in figure 10 represent results of the initial and final values of the maximum WRBM. In all cases, at each value of k, the lower symbols represent the initial value of maximized WRBM and the upper symbols represent the final value. Regardless of the starting point, the direct optimizer consistently achieved the same value of maximized WRBM, indicating that it was more insensitive to the starting point than

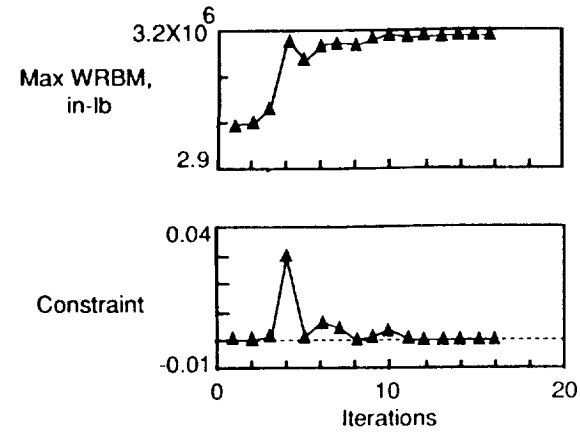

Figure 8.- Convergence history for maximizing WRBM of the rigid model using the direct optimizer and 54 Chebyshev polynomials.

was the indirect optimizer. The direct optimizer also yielded larger maximum load values and converged in fewer iterations. In addition, the direct optimizer was able to converge with both Chebyshev and cubic spline approximations to the excitation waveform while the indirect optimizer was not able to converge when the spline approximation was used.

In figure 10 the lower gray squares are below the solid line but the upper gray squares are very close to the highest value of WRBM achieved. The lower symbols being below the solid line is due to the fact that the spline approximation does a poorer job at reproducing the initial excitation waveform than does the Chebyshev approximation. However, the spline approximation does a very adequate job of reproducing the final excitation waveform and produces maximized WRBMs very close to those produced by the Chebyshev approximation.

From the data presented in figure 10, the usefulness and value of the one-dimensional search procedure becomes obvious. A very simple and straightforward variation in a single quantity, k, produced a value of maximized load which is within 1.1% of the value produced by the significantly more complex multi-dimensional search procedure.

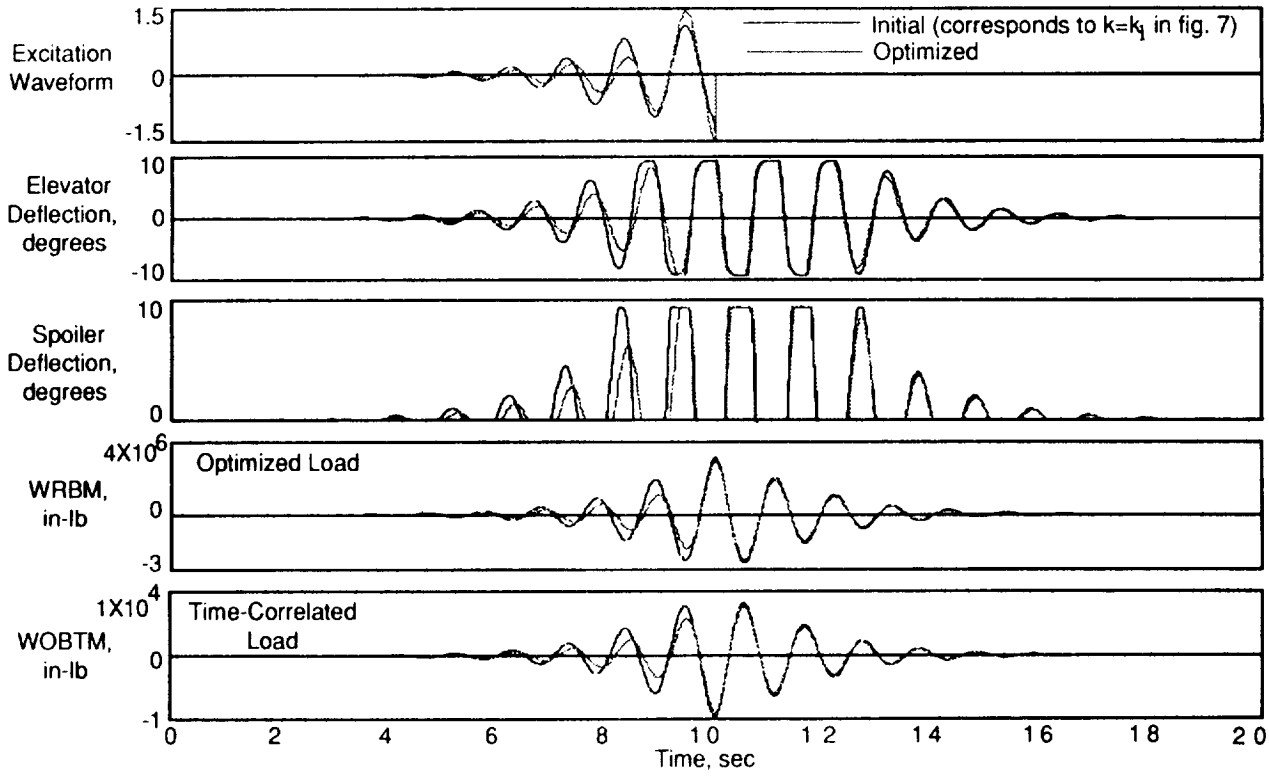

Figure 9.- Comparison of initial and optimized time-histories. Rigid model.

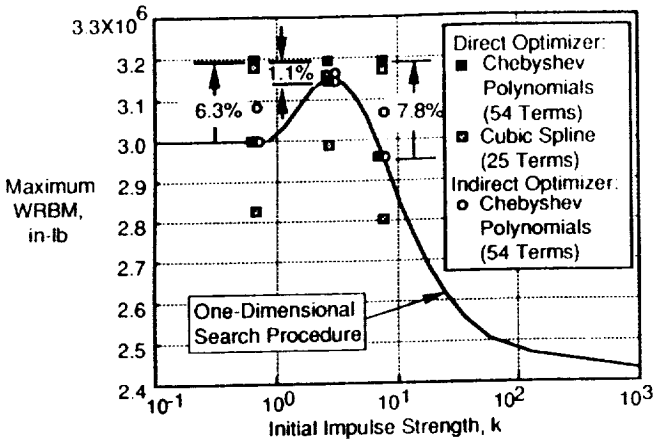

Figure 10.- Summary of results for maximizing WRBM using the one-dimensional and several multi-dimensional searches. Rigid model.

Figure 11 shows results for maximizing WRBM using the flexible model. The solid line again represents results from the one-dimensional search procedure and the squares represent results from the multi-dimensional search. In this example, because of the higher-frequency dynamics in the excitation waveform, 124 Chebyshev polynomials were required to produce an adequate approximation of the waveform. The indirect optimizer was not considered here for the reasons cited above. Also, the spline approximation was unsuccessful for this model, even with the direct optimizer. Consistent results were obtained for the flexible model only when the direct optimizer and the Chebyshev polynomial approximation were used.

The usefulness and value of the one-dimensional search procedure is again illustrated by the results from figure 11. The simple procedure produced a value of maximized load which is within 0.78% of the value produced by the multi-dimensional search procedure.

So far, the only load considered has been wing root bending moment. Figure 12 shows results for maximizing wing outboard torsion moment (WOBTM) for the flexible model. The solid line represents results from applying the one-dimensional search procedure to WOBTM. The general shapes of the solid lines in figures 10, 11, and 12 are very similar. For the multi-dimensional search procedure, 220 Chebyshev polynomials

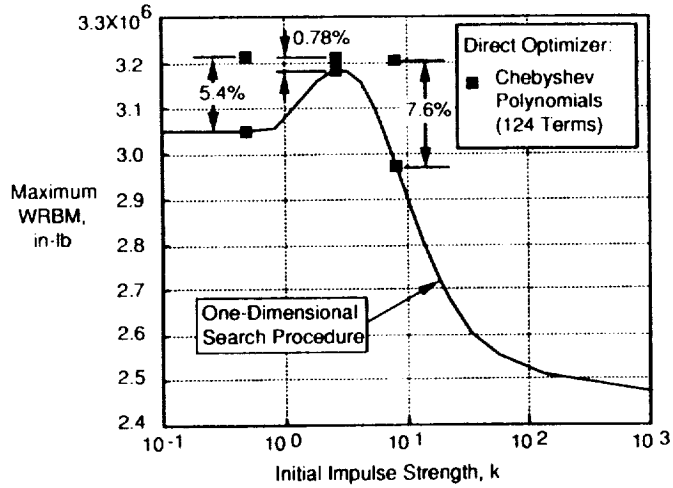

Figure 11.- Summary of results for maximizing WRBM using the one-dimensional and several multi-dimensional searches. Flexible model.

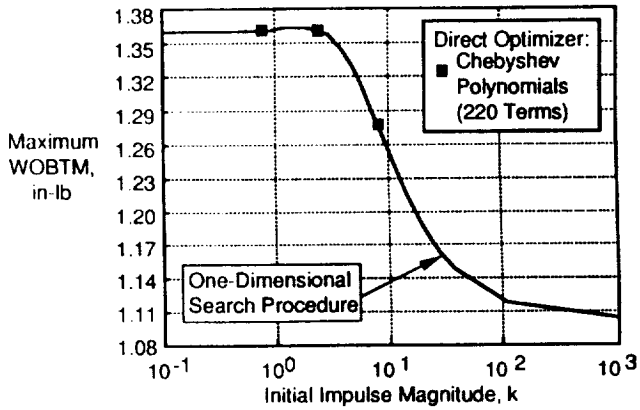

Figure 12.- Summary of results for maximizing WOBTM using the one-dimensional and several multi-dimensional searches. Flexible model.

were required to produce an adequate approximation of the excitation waveform. The solid squares represent only the initial values of maximized WOBTM; final values are not shown because, due to the large number of coefficients, a converged solution was not obtained.

Based on the ability (demonstrated in figures 10 and 11) of the one-dimensional search procedure to produce maximized loads very close to those produced by the multi-dimensional search procedure, it is the opinion of the authors that the value of the maximum WOBTM is very close to the value predicted by the one-dimensional search.

Concluding Remarks

This paper has presented two search procedures (one-dimensional and multi-dimensional) for obtaining maximized gust loads for a nonlinear airplane using Matched Filter Theory and constrained optimization. The procedures were applied to an example airplane with a nonlinear gust load alleviation active control system. Numerical results confirm that the procedures are successful in maximizing the loads of interest. For the example configuration considered, the one-dimensional search succeeded in obtaining loads that were within about 1% of the loads produced by the multi-dimensional search procedure. This suggests that the simpler one-dimensional search method may be the most practical implementation. In addition, further study is required of the modelling of excitation waveforms characterized by high-frequency contents.

References

1. Jones, J. G.: Statistical-Discrete-Gust Method for Predicting Aircraft Loads and Dynamic Response. Journal of Aircraft, Vol. 26, No. 4, April 1989, pp. 382-392.

2. Pototzky, A. S.; Zeiler, T. A.; and Perry III, B.: Time-Correlated Gust Loads Using Matched-Filter Theory and Random Process Theory - A New Way of Looking at Things. NASA TM-101573, April 1989.

3. Barnes, Terence J.: Harmonization of U.S. and European Gust Criteria for Transport Aircraft. Proceedings of the 17th Congress of the International Council of the Aeronautical Sciences, Stockholm, Sweden, September 9-14, 1990, pp. 586-593.

4. Pototzky, A. S.; Heeg, J.; and Perry, B., III: Computation of Maximum Gust Loads in Nonlinear Aircraft Using a New Method Based on the Matched Filter Approach and Numerical Optimization. Work-in-Progress paper presented at the AIAA/ASME/ASCE/AHS/ASC 31st Structures, Structural Dynamics and Materials Conference, Long Beach, California, April 2-4, 1990.

5. Schittkowski, K.: NLPQL: A FORTRAN Subroutine Solving Constrained Nonlinear Programming Problems. Annals of Operations Research 5, 1985-1986, pp. 485-500.

6. Wrenn, G. A.: An Indirect Method for Numerical Optimization Using the Kreisselmeier-Steinhauser Function. NASA Contractor Report 4220, 1989.

7. SYSTEM_BUILD 7.0 User's Guide: Integrated Systems Inc., October, 1988.

8. HYPER_BUILD 7.0 User's Guide: Integrated Systems Inc. October, 1988.

9. Giesing, J. P.; Kalman, T. P.; and Rodden, W. P.: Subsonic Unsteady Aerodynamics for General Configurations, Part I: Direct Application for the Nonplanar Doublet Lattice Method. AFFDL-TR-71-5, 1971.

10. Mukhopadhyay, V.: Digital Robust Control Law Synthesis Using Constrained Optimization. Journal of Guidance, Control and Dynamics, Vol. 12, No. 2, March-April 1989, pp. 175-181.

NASA

Report Documentation Page

1. Report No.	2. Government Accession No.	3. Recipient's Catalog No.
NASA TM-104138		

4. Title and Subtitle

Maximized Gust Loads for a Nonlinear Airplane Using Matched Filter Theory and Constrained Optimization

5. Report Date

September 1991

6. Performing Organization Code

7. Author(s)

Robert C. Scott
Anthony S. Pototzky
Boyd Perry III

8. Performing Organization Report No.

10. Work Unit No.

505-63-50-15

9. Performing Organization Name and Address

NASA Langley Research Center
Hampton, VA 23665-5225

11. Contract or Grant No.

13. Type of Report and Period Covered

Technical Memorandum

12. Sponsoring Agency Name and Address

National Aeronautics and Space Administration
Washington, DC 20546-0001

14. Sponsoring Agency Code

15. Supplementary Notes

This paper was presented at the 1991 AIAA Atmospheric Flight Mechanics Conference, August 19-21, 1991, New Orleans, Louisiana.

16. Abstract

This paper describes and illustrates two matched-filter-theory based schemes for obtaining maximized and time-correlated gust-loads for a nonlinear airplane. The first scheme is computationally fast because it uses a simple one-dimensional search procedure to obtain its answers. The second scheme is computationally slow because it uses a more complex multi-dimensional search procedure to obtain its answers, but it consistently provides slightly higher maximum loads than the first scheme. Both schemes are illustrated with numerical examples involving a nonlinear control system.

17. Key Words (Suggested by Author(s))

Matched Filter Theory
Gust Loads
Dynamic Loads
Nonlinear Model
Time-Correlated Loads

18. Distribution Statement

Unclassified - Unlimited

Subject Category - 05

19. Security Classif. (of this report)	20. Security Classif. (of this page)	21. No. of pages	22. Price
Unclassified	Unclassified	10	A02